Simple and efficient algorithms based on Volterra equations to compute memory kernels and projected cross-correlation functions from molecular dynamics

Amaël Obliger

Simple and efficient algorithms based on Volterra equations to compute memory kernels and projected cross-correlation functions from molecular dynamics

Amaël Obliger[1, a)]
Institut des Sciences Moléculaires, Univ. of Bordeaux – Bordeaux INP – CNRS, UMR 5255, F-33400 Talence, France

(Dated: 13 March 2023)

Starting from the orthogonal dynamics of any given set of variables with respect to the projection variable used to derive the Mori-Zwanzig equation, a set of coupled Volterra equations is obtained that relate the projected time correlation functions between all the variables of interest. This set of equations can be solved using standard numerical inversion methods for Volterra equations, leading to a very convenient yet efficient strategy to obtain any projected time correlation function or contribution to the memory kernel entering a generalized Langevin equation. Using this strategy, the memory kernel related to the diffusion of tagged particles in a bulk Lennard-Jones fluid is investigated up to the long-term regime to show that the repulsive-attractive cross contribution to memory effects represents a small but non-zero contribution to the self-diffusion coefficient.

I. INTRODUCTION

Because of the large number of degrees of freedom involved in stochastic systems we use coarse-graining procedures where few observables are selected to describe the systems' evolution. The dynamics of such coarse-grained, or macroscopic, variables is filtered out of the dynamics of the other "irrelevant" microscopic variables which constitute the environment of the formers. In the Langevin equation, this is achieved by splitting the coarse-grained dynamics into two components, a random one summing up the interactions with the environment, and a dissipative one representing the response of the macroscopic variables to their environment. The Markovian assumption is made where the dynamics of the microscopic degrees of freedom occur on a negligible timescale compared to the characteristic one of the macroscopic dynamics. Such an assumption is removed in the Mori-Zwanzig equation[1–3] that becomes important as the separation of timescales is incomplete. Those memory effects are quantified by memory kernels or, more generally, by projected time correlation functions if one is also interested in decomposing memory kernels or in the coupling between different macroscopic variables.

Despite the difficulty of such a task, the calculation of memory kernels from microscopic dynamics can be performed reliably and efficiently by inverting the Volterra equations obtained from the Generalized Langevin Equation (GLE)[4–14], although more complex methods exist[15–20]. The simple yet efficient method based on the inversion of Volterra equations has, however, only been applied to the computation of the memory kernel appearing in the GLE. Also, the first numerical method allowing to decompose the memory kernel, or more generally to compute projected correlation functions, has been proposed quite recently by Carof *et al.*[21] and is based on the reconstruction of the random force, which obeys an "orthogonal" dynamics. In particular, it permitted the authors to investigate the diffusive dynamics of a tagged particle in a bulk Lennard-Jones (LJ) fluid by decomposing the memory kernel into contributions pertaining to the repulsive and attractive parts of the LJ interactions. Similarly, the dynamics of ions confined in a clay nanopore has been studied by separating the ion-ion, ion-clay, and ion-water interactions[22].

Here, Volterra equations are derived within Mori's projection operator formalism from the orthogonal dynamics of generic variables that form a set of coupled equations for the projected time correlation functions between the variables themselves and between the variables and the specific variable onto which the dynamics is projected. Then, these Volterra equations can be reliably inverted using simple numerical integration schemes to provide any projected time correlation functions or memory kernels. Such a strategy proves to be more convenient and less computationally intensive than the method based on the reconstruction of the orthogonal dynamics of the considered variables as Volterra equations inversion only requires time correlation functions. This is demonstrated by investigating the diffusive dynamics of a tagged particle in a LJ fluid following the repulsive-attractive decomposition of the LJ interactions for the memory kernel related to the self-diffusion coefficient. The efficiency of such a strategy made it possible to quantitatively assess the different long-term contributions for the first time.

In the following, the projection operator formalism is first recalled, as well as the numerical scheme based on the inversion of the Volterra equation associated with the GLE to compute its memory kernel. Then, the set of coupled Volterra equations needed to generalize the latter procedure for any projected correlation functions for the Mori equation is derived from the orthogonal dynam-

[a)] amael.obliger@u-bordeaux.fr

ics, and the numerical method strategy to solve them is given. A simple derivation of the orthogonal dynamics of any variable is also provided. Finally, the dynamics of a bulk LJ fluid is investigated at all times according to the repulsive-attractive decomposition of the LJ potential by applying the new strategy to trajectories obtained by classical Molecular Dynamics (MD) simulations.

II. PROJECTION OPERATOR FORMALISM

A. Mori's Projection Operator

Within the projection operator formalism, one wants to describe systems composed of many degrees of freedom by focusing on a few *relevant*, *macroscopic* or *slow* variables. We consider Hamiltonian systems described through a set $q = (q_i)_{i\in[1,n_d]}$ of n_d classical microscopic degrees of freedom with their respective momenta $p = (p_i)_{i\in[1,n_d]}$ that evolve in time as

$$\dot{q}_i(t) = \frac{\partial \mathcal{H}(\Gamma_t)}{\partial p_i} \tag{1}$$

$$\dot{p}_i(t) = -\frac{\partial \mathcal{H}(\Gamma_t)}{\partial q_i} \tag{2}$$

where $\mathcal{H}$ is the Hamiltonian operator acting on a phase space frame $\Gamma_t = (q_i(t), p_i(t))_{i\in[1,n_d]}$ at time t, and the dot denotes the total time derivative. For any variable A, its time evolution then obeys

$$\dot{\mathrm{A}}(t) = i\mathcal{L}\mathrm{A}(t) \tag{3}$$

where $i\mathcal{L}$ is the Liouvillian operator defined by its action on a variable A as $i\mathcal{L}\mathrm{A}(t) = -\{\mathcal{H}, \mathrm{A}(t)\}$ with $\{\cdot,\cdot\}$ the Poisson brackets. The variable A is also an operator that acts on the phase space frames Γ_t with the restriction that this operator does not evolve in time, i.e., it is a function of the microscopic degrees of freedom that does not explicitly depend on time. The formal solution of the previous equation reads

$$\mathrm{A}(t) = \mathrm{e}^{i\mathcal{L}t}\,\mathrm{A}(0) \tag{4}$$

where $t = 0$ has been taken as the initial time.

In Mori's operator formalism, we choose a macroscopic variable P to describe the evolution of the system while integrating out the other microscopic degrees of freedom. This is formally accomplished by the action of a projector $\mathcal{P}$ that projects any variable X onto the macroscopic variable P as

$$\mathcal{P}\mathrm{X} = \frac{\langle \mathrm{X}(0)\mathrm{P}(0)\rangle}{\langle \mathrm{P}(0)^2\rangle}\mathrm{P}(0)\,. \tag{5}$$

The bracket notation $\langle\cdot\rangle$ corresponds to the ensemble averaging at equilibrium over Hamiltonian trajectories following Eqs. 1 and 2. The remaining "irrelevant" degrees of freedom are then projected out via the orthogonal operator $\mathcal{Q} = I - \mathcal{P}$, where I is the identity operator. Applying Dyson's operator identity

$$\mathrm{e}^{i\mathcal{L}t} = \int_0^t \mathrm{e}^{i\mathcal{L}(t-s)}\,\mathcal{P}i\mathcal{L}\,\mathrm{e}^{i\mathcal{Q}\mathcal{L}s}\,\mathrm{d}s + \mathrm{e}^{i\mathcal{Q}\mathcal{L}t} \tag{6}$$

to the time derivative $\dot{\mathrm{A}}(t) = i\mathcal{L}\,\mathrm{e}^{i\mathcal{L}t}\,\mathrm{A}(0)$ of an observable A and decomposing the last term as $\mathrm{e}^{i\mathcal{Q}\mathcal{L}t} = \mathrm{e}^{i\mathcal{Q}\mathcal{L}t}(\mathcal{P}+\mathcal{Q})$ leads to the so-called Mori-Zwanzig equation

$$\dot{\mathrm{A}}(t) = \Omega\mathrm{P}(t) - \int_0^t K(s)\mathrm{P}(t-s)\,\mathrm{d}s + \mathrm{R}(t) \tag{7}$$

with the drift term

$$\Omega = \frac{\langle \dot{\mathrm{A}}(0)\mathrm{P}(0)\rangle}{\langle \mathrm{P}(0)^2\rangle}\,, \tag{8}$$

the memory kernel

$$K(t) = \frac{\langle \mathrm{R}(t)\dot{\mathrm{P}}(0)\rangle}{\langle \mathrm{P}(0)^2\rangle}\,, \tag{9}$$

and the noise

$$\mathrm{R}(t) = \mathrm{e}^{i\mathcal{Q}\mathcal{L}t}\,\mathcal{Q}\dot{\mathrm{A}}(0)\,. \tag{10}$$

Such equations can be generalized for a collection of n_p relevant variables $(\mathrm{P}_i)_{i\in[1,n_p]}$ transforming Eqs. 7 and 10 into vectors and Eqs. 8 and 9 into matrices[2,23].

By definition, the noise R is decorrelated from the relevant variable P at all times ($\langle \mathrm{R}(t)\mathrm{P}(0)\rangle = 0$), and its time correlation with the time derivative of the relevant variable defines the memory kernel, which encodes the delayed effects of all the other degrees of freedom orthogonal to P on the dynamics of the observable A. Evaluating the drift term (Eq. 8) from the Hamiltonian dynamics of the systems is as straightforward as evaluating the denominator $\langle \mathrm{P}(0)^2\rangle$, as opposed to the noise or the memory kernel.

B. Generalized Langevin Equation

Taking the relevant observable P as the velocity v of a tagged particle and A as its momentum mv with m the particle mass, one gets the usual generalized Langevin equation

$$m\dot{v}(t) = -\int_0^t k(s)v(t-s)\,\mathrm{d}s + \eta(t) \tag{11}$$

with $\eta(t) = \mathrm{e}^{i\mathcal{Q}\mathcal{L}t}\,f(0)$, $f(t)$ the total force acting on the particle, and the friction kernel

$$k(t) = \frac{\langle \eta(t)\eta(0)\rangle}{k_B T}\,, \tag{12}$$

by noting that the force f is orthogonal to the relevant variable v ($\mathcal{P}f = 0$), and that $\langle v(0)^2\rangle = k_B T/m$ at thermal equilibrium. By choosing to consider the dynamics of

a variable A proportional to the relevant variable, leading to $\mathcal{P}\mathrm{A} = \mathrm{A}$, the memory kernel becomes the time auto-correlation of the noise. In the Markovian approximation, the timescale of the dynamics of the velocity is well separated from the ones of the microscopic degrees of freedom, and the memory kernel can simply be considered as a Dirac pulse, bringing us back to the Langevin equation $m\dot{v}(t) = -\gamma v(t) + \eta(t)$.

One efficient and simple way to numerically estimate the memory kernel (Eq. 12) from the dynamics of the system is to take the ensemble average of Eq. 11 after multiplying it by $v(0)$, which leads to a Volterra equation of the first kind

$$m\langle \dot{v}(t)v(0)\rangle = -\int_0^t k(s)\langle v(t-s)v(0)\rangle \,\mathrm{d}s \tag{13}$$

after noting that $\langle \eta(t)v(0)\rangle = 0$ due to the orthogonal dynamics of the noise. As noted in[8], numerically inverting this equation is not stable. Instead, its time derivative

$$-m\langle \dot{v}(t)\dot{v}(0)\rangle = -\frac{k_BT}{m}k(t) - \int_0^t k(s)\langle \dot{v}(t-s)v(0)\rangle \,\mathrm{d}s\,, \tag{14}$$

a Volterra equation of the second kind, should be considered. Rewriting this expression as function of the total force $f(t) = m\dot{v}(t)$ and introducing the notation $C^{XY}(t) = \langle X(t)Y(0)\rangle$ gives

$$C^{ff}(t) = k_BTk(t) + \int_0^t k(s)C^{fv}(t-s)\,\mathrm{d}s\,. \tag{15}$$

This equation can be discretized in time using the trapezoidal rule for the integral as

$$C_i^{ff} = k_BTk_i + \sum_{j=0}^{i}\psi_j k_j C_{i-j}^{fv}\delta t\,, \tag{16}$$

where δt is the time resolution, $\psi_j = 1 - 0.5\delta_{0j}$, and all the time-dependent functions g have been discretized as $g_i = g(i\delta t)$ with $i \in [0, n_t - 1]$, n_t being the total number of time-frames along the trajectory. Because $C_0^{fv} = 0$, a very simple iterative scheme can thus be obtained as

$$k_i = \frac{C_i^{ff} - \delta t\sum_{j=0}^{i-1}\psi_j k_j C_{i-j}^{fv}}{k_BT}\,. \tag{17}$$

This algorithm only requires the averaged time auto-correlation function of the force and the averaged force-velocity time correlation function. Such correlation functions can be very efficiently computed with an $\mathcal{O}(n_t \ln n_t)$ complexity by using the Wiener-Khintchine theorem[24,25]. Despite being efficient and simple to implement, this approach based on the discretization of a Volterra equation of the second kind has been restricted[19,21] to the evaluation of the memory kernel where the observable under consideration A is proportional to the relevant variable P, i.e., when the memory kernel is determined by the noise auto-correlation function. We will see later that this restriction can be removed.

C. Orthogonal Time Correlation Functions

Returning to the memory kernel (Eq. 9) of the Mori equation, we note that it implies in the general case to evaluate the time cross-correlation function of $\dot{\mathrm{P}}$ and the orthogonal dynamics of $\dot{\mathrm{A}}$. Expanding Eq. 9 with the definition of the noise (Eq. 10), the memory kernel reads

$$K(t) = \frac{\langle \dot{\mathrm{P}}(0)\,\mathrm{e}^{i\mathcal{Q}\mathcal{L}t}\,\mathcal{Q}\dot{\mathrm{A}}(0)\rangle}{\langle \mathrm{P}(0)^2\rangle}\,. \tag{18}$$

Since the noise does not follow a Hamiltonian dynamics but an orthogonal one, it cannot be directly extracted from the system dynamics, nor can it be propagated in time by the numerical integrators used in MD calculations. To circumvent this problem, Carof et al.[21] derived two algorithms that reconstruct the noise or the orthogonal dynamics of any observable, say M, and thus allow one to compute its time correlation with any other observable, say N, as

$$\bar{C}^{\mathrm{MN}}(t) = \langle \mathrm{N}(0)\,\mathrm{e}^{i\mathcal{Q}\mathcal{L}t}\,\mathrm{M}(0)\rangle\,. \tag{19}$$

Noting from[26] that the adjoint of $\mathrm{e}^{i\mathcal{Q}\mathcal{L}t}$ is $\mathrm{e}^{-i\mathcal{L}\mathcal{Q}t}$ for the ensemble average $\langle\cdot\rangle$ understood as a scalar product in the operator space, we also have

$$\bar{C}^{\mathrm{MN}}(t) = \langle \mathrm{M}(0)\,\mathrm{e}^{-i\mathcal{L}\mathcal{Q}t}\,\mathrm{N}(0)\rangle\,. \tag{20}$$

From the two previous expressions, two observables naturally appear, $\mathrm{M}^+(t) = \mathrm{e}^{i\mathcal{Q}\mathcal{L}t}\,\mathrm{M}(0)$ and $\mathrm{N}^-(t) = \mathrm{e}^{-i\mathcal{L}\mathcal{Q}t}\,\mathrm{N}(0)$, following a forward (+) or a backward (−) orthogonal dynamics given by

$$\dot{\mathrm{M}}^+(t) = i\mathcal{L}\mathrm{M}^+(t) - \mathcal{P}i\mathcal{L}\mathrm{M}^+(t)\,, \tag{21}$$

$$\dot{\mathrm{N}}^-(t) = -i\mathcal{L}\mathrm{N}^-(t) + i\mathcal{L}\mathcal{P}\mathrm{N}^-(t)\,, \tag{22}$$

respectively. Both orthogonal dynamics differ from the Hamiltonian one ($\dot{\mathrm{A}}(t) = i\mathcal{L}\mathrm{A}(t)$). Such projected correlation functions can be either expressed as

$$\bar{C}^{\mathrm{MN}}(t) = C^{\mathrm{M}^+\mathrm{N}}(t) = \langle \mathrm{M}^+(t)\mathrm{N}(0)\rangle\,, \tag{23}$$

or as

$$\bar{C}^{\mathrm{MN}}(t) = C^{\mathrm{N}^-\mathrm{M}}(t) = \langle \mathrm{N}^-(t)\mathrm{M}(0)\rangle\,. \tag{24}$$

Note that, in general, the time correlation function $\bar{C}^{\mathrm{MN}}(t)$ is not stationary in time, even though the microscopic dynamics is time reversible. However, for the generalized Langevin equation, the memory kernel is stationary, as demonstrated in[21]. Indeed, stationarity is recovered when both observables M and N are orthogonal to the relevant variable P, i.e., when $\mathrm{M} = \mathcal{Q}\mathrm{M}$ and $\mathrm{N} = \mathcal{Q}\mathrm{N}$. Upon inspection of the orthogonal dynamics of both variables M^+ and N^-, Carof et al.[21] shown that the time derivative of auxiliary observables, defined as $\hat{\mathrm{M}}^+(t) = \mathrm{e}^{-i\mathcal{L}t}\,\mathrm{M}^+(t)$ and $\hat{\mathrm{N}}^-(t) = \mathrm{e}^{i\mathcal{L}t}\,\mathrm{N}^-(t)$, can

be simply expressed using a time-dependent operator $\mathcal{P}_t = \mathrm{e}^{i\mathcal{L}t}\,\mathcal{P}\,\mathrm{e}^{-i\mathcal{L}t}$ as

$$\dot{\hat{\mathrm{M}}}^{+}(t) = -\mathcal{P}_{-t} i\mathcal{L}\hat{\mathrm{M}}^{+}(t)\,, \tag{25}$$

$$\dot{\hat{\mathrm{N}}}^{-}(t) = i\mathcal{L}\mathcal{P}_t\hat{\mathrm{N}}^{-}(t)\,. \tag{26}$$

Following some algebraic calculations detailed in[21], such expressions can be formally integrated to give the central relations

$$\mathrm{M}^{+}(t) = \mathrm{M}(t) + \int_0^t \frac{\langle \mathrm{M}^{+}(s)\dot{\mathrm{P}}(0)\rangle}{\langle \mathrm{P}(0)^2\rangle}\mathrm{P}(t-s)\,\mathrm{d}s\,, \tag{27}$$

$$\mathrm{N}^{-}(t) = \mathrm{N}(-t) + \int_0^t \frac{\langle \mathrm{N}^{-}(s)\mathrm{P}(0)\rangle}{\langle \mathrm{P}(0)^2\rangle}\dot{\mathrm{P}}(s-t)\,\mathrm{d}s\,. \tag{28}$$

Note the main difference between both expressions, the integral term for the backward dynamics involves a correlation function between the orthogonal dynamics of the observable and the relevant variable, not its time derivative as for the forward dynamics (and the Volterra equation derived from the GLE Eq. 13).

Also, alternatively to the derivation of the Forward Orthogonal Dynamics (FOD) just recalled, one can directly apply the Dyson operator identity (Eq. 6) to the variable M, showing that the dynamics of the orthogonal time quantity M^{+} (Eq. 27) directly follows from Duhamel's principle[27]. Interestingly, the same observation can be made for the backward orthogonal dynamics $\mathrm{N}^{-}(t) = \mathrm{e}^{-i\mathcal{L}\mathcal{Q}t}\,\mathrm{N}(0)$ for which the order of $i\mathcal{L}$ and $\mathcal{Q}$ is reversed compared to Dyson's identity. Inverting those operators in the Dyson identity leads to

$$\mathrm{e}^{i\mathcal{L}t} = \int_0^t \mathrm{e}^{i\mathcal{L}(t-s)}\,i\mathcal{L}\mathcal{P}\,\mathrm{e}^{i\mathcal{L}\mathcal{Q}s}\,\mathrm{d}s + \mathrm{e}^{i\mathcal{L}\mathcal{Q}t}\,, \tag{29}$$

which, upon the changes of variables $t \to -t$ and $s \to -s$, gives the operator identity

$$\mathrm{e}^{-i\mathcal{L}t} = -\int_0^t \mathrm{e}^{-i\mathcal{L}(t-s)}\,i\mathcal{L}\mathcal{P}\,\mathrm{e}^{-i\mathcal{L}\mathcal{Q}s}\,\mathrm{d}s + \mathrm{e}^{-i\mathcal{L}\mathcal{Q}t} \tag{30}$$

that can be applied to the observable N to retrieve Eq. 28 in a direct manner.

Before discretizing Eqs. 27 and 28, one important point should be raised. Contrary to the Hamiltonian dynamics, the orthogonal dynamics is not stationary in time. This is best clarified by temporarily stating the time point from which the orthogonal dynamics is propagated, considering an initial time t_0, the orthogonal dynamics of M after a duration Δt is denoted by $\mathrm{M}^{+}(\Delta t)[\Gamma_{t_0}]$ and is not equal to $\mathrm{M}^{+}(t_0+\Delta t)[\Gamma_0]$ the orthogonal dynamics propagated from $t = 0$ to $t_0 + \Delta t$. It is otherwise the case for the Hamiltonian dynamics, i.e., $\mathrm{M}(\Delta t)[\Gamma_{t_0}] = \mathrm{M}(t_0+\Delta t)[\Gamma_0]$. For instance, the previous expression for the FOD (Eq. 27) can be expressed as

$$\mathrm{M}^{+}(t)[\Gamma_0] = \mathrm{M}(t)[\Gamma_0] + \int_0^t \frac{C^{\mathrm{M}^{+}\dot{\mathrm{P}}}(s)}{\langle \mathrm{P}(0)^2\rangle}\mathrm{P}(t-s)[\Gamma_0]\,\mathrm{d}s\,, \tag{31}$$

which, after some manipulations[21], leads to

$$\mathrm{M}^{+}(t+\delta t)[\Gamma_0] = \mathrm{M}^{+}(t)[\Gamma_{\delta t}] + \int_0^{\delta t} \frac{C^{\mathrm{M}^{+}\dot{\mathrm{P}}}(t+s)}{\langle \mathrm{P}(0)^2\rangle}\mathrm{P}(-s)[\Gamma_{\delta t}]\,\mathrm{d}s\,. \tag{32}$$

This expression can then be discretized without ambiguity by employing the rectangle rule, leading to an algorithm with first order w.r.t the timestep δt as

$$\mathrm{M}^{+}_{i+1}[l] = \mathrm{M}^{+}_{i}[l+1] + \beta_i \mathrm{P}_{l+1}\delta t\,, \tag{33}$$

where the index l runs between 0 and $n_t - i - 1$, and with

$$\beta_i = \frac{\sum_{m=0}^{n_t-i-1}\dot{\mathrm{P}}_m \mathrm{M}^{+}_i[m]}{\sum_{m=0}^{n_t-i-1}\mathrm{P}_m^2}\,, \tag{34}$$

where the specific notation in square brackets has been dropped for stationary quantities only. At each iteration i, the projected time correlation function Eq. 19 can be computed as

$$C_i^{\mathrm{M}^{+}\mathrm{N}} = \frac{1}{n_t - i}\sum_{m=0}^{n_t-i-1}\mathrm{N}_m \mathrm{M}^{+}_i[m]\,, \tag{35}$$

which corresponds to a running average over all the possible trajectory segments of time $i\delta t$ for which the orthogonal dynamics has been reconstructed. This first-order algorithm, initially derived by Carof et al.[21], was later improved by Lesnicki et al.[28] using the trapezoidal rule to reach second-order accuracy in δt, leading to a numerically more stable algorithm at little extra computational cost. In the following, unless explicitly stated, only the second-order algorithm of the FOD is concerned when referring to the reconstruction algorithm.

For a bulk LJ fluid, the initial algorithms were notably the first to allow, (i) the study of the noise distribution – showing that it is non-Gaussian, as for the force distribution, and that the distribution of the difference between noise and force is Gaussian –, and (ii) the decomposition of the memory kernel – showing that the repulsive part of the LJ potential dominates the friction coefficient $\gamma = \int_0^\infty k(s)\mathrm{d}s$.

In practice, the reconstruction of the orthogonal dynamics is performed for each available trajectory (particle) of the system dynamics, and the correlation functions are averaged over those trajectories. Finally, the complexity of such algorithms goes as $\mathcal{O}(n_t n_c)$ with n_c corresponding to the maximum duration $n_c\delta t$ over which the correlation function is investigated. This maximum time is, of course, determined by the physics of the system at hand and should be large enough to encompass the complete relaxation of the memory effects. Also, it is to be noted that, since the strategy of such reconstruction algorithms is to propagate the orthogonal dynamics, the time resolution needed is the same as that used in MD to generate the Hamiltonian dynamics.

So far, we have two numerical strategies to investigate memory effects: one based on the solution of the

Volterra equation of the second kind (Eq. 15), and one based on the reconstruction of the orthogonal dynamics (Eq. 32). The former allows to efficiently compute the memory kernel by leveraging the Wiener-Khintchine theorem to compute first the TCFs needed with $\mathcal{O}(n_t \ln n_t)$ complexity and then to invert the Volterra equation that needs to be done only once for all the individual trajectories over which the TCFs have been averaged, but not allowing to compute orthogonal cross-correlations, which is required to decompose the memory kernel over multiple contributions. Reconstructing the orthogonal dynamics allows such calculations, but at the price of propagating the orthogonal dynamics ($\mathcal{O}(n_t n_c)$) for each trajectory available before averaging. Moreover, when solving the Volterra equation, the time resolution can be lower than the one used to generate the MD trajectories, but needs to be large enough to allow for an accurate integration of the memory kernel if one wants the friction coefficient. We will see later that the resolution needed depends on the dynamics of the memory effects themselves. We now turn to the reconciliation between the two approaches to get the best of both worlds.

D. Volterra Equations for Projected Cross-Correlation Functions

Here and in what follows, the Volterra equation refers exclusively to the second kind. A couple of observations are in order before going further. The usual derivation of the Volterra equation (15) consists of multiplying the GLE by the velocity, then taking the time derivative of the ensemble average. It implies that decomposing the memory kernel over different contributions would be possible only by decomposing the velocity in the same way, which is not possible. Alternatively to this derivation of the Volterra equation and more straightforwardly, one can simply multiply the GLE by the force $f(0)$ instead of the velocity, and take the ensemble average. This will be generalized in order to obtain a suitable set of Volterra equations, allowing us to reliably evaluate the projected correlation functions. Let us consider a set of n_o observables $(\mathrm{B}_\alpha)_{\alpha\in[1,n_o]}$ for which one wants to compute their projected correlation functions

$$C^{\mathrm{B}_\alpha^+\mathrm{B}_\beta^+}(t) = \langle \mathrm{B}_\alpha^+(t)\mathrm{B}_\beta^+(0)\rangle \;\; \forall \alpha,\beta \in [1,n_o]\,. \tag{36}$$

Using Eq. 27 for B_α and taking its average after multiplying by $\mathrm{B}_\beta^+(0) = \mathrm{B}_\beta(0)$, one arrives at

$$\langle \mathrm{B}_\alpha^+(t)\mathrm{B}_\beta^+(0)\rangle = \langle \mathrm{B}_\alpha(t)\mathrm{B}_\beta(0)\rangle + \int_0^t \frac{\langle \mathrm{B}_\alpha^+(s)\dot{\mathrm{P}}(0)\rangle}{\langle \mathrm{P}(0)^2\rangle}\langle \mathrm{P}(t-s)\mathrm{B}_\beta(0)\rangle\,\mathrm{d}s\,, \tag{37}$$

which is a Volterra equation of the second kind but involving the yet unknown projected correlation function $C^{\mathrm{B}_\alpha^+\dot{\mathrm{P}}}(t)$ in the integral, as opposed to the time correlation functions $C^{\mathrm{B}_\alpha\mathrm{B}_\beta}(t)$ and $C^{\mathrm{PB}_\beta}(t)$, which can be obtained efficiently from MD trajectories. Now, the same step is repeated but with $\dot{\mathrm{P}}(0)$ to get a Volterra equation for the required $C^{\mathrm{B}_\alpha^+\dot{\mathrm{P}}}(t)$ as

$$\langle \mathrm{B}_\alpha^+(t)\dot{\mathrm{P}}(0)\rangle = \langle \mathrm{B}_\alpha(t)\dot{\mathrm{P}}(0)\rangle + \int_0^t \frac{\langle \mathrm{B}_\alpha^+(s)\dot{\mathrm{P}}(0)\rangle}{\langle \mathrm{P}(0)^2\rangle}\langle \mathrm{P}(t-s)\dot{\mathrm{P}}(0)\rangle\,\mathrm{d}s\,. \tag{38}$$

Again, $C^{\mathrm{B}_\alpha\dot{\mathrm{P}}}(t)$ and $C^{\mathrm{P}\dot{\mathrm{P}}}(t)$ can be evaluated from MD trajectories, but this Volterra equation can be numerically inverted as

$$C_i^{\mathrm{B}_\alpha^+\dot{\mathrm{P}}} = C_i^{\mathrm{B}_\alpha\dot{\mathrm{P}}} + \delta t \sum_{j=0}^{i-1} \psi_j C_j^{\mathrm{B}_\alpha^+\dot{\mathrm{P}}} C_{i-j}^{\mathrm{P}\dot{\mathrm{P}}}/C_0^{\mathrm{PP}}\,, \tag{39}$$

since $C_0^{\mathrm{P}\dot{\mathrm{P}}} = 0$, following the same procedure as for Eq. 15. Then, Eq. 37 can be numerically integrated as

$$C_i^{\mathrm{B}_\alpha^+\mathrm{B}_\beta^+} = C_i^{\mathrm{B}_\alpha\mathrm{B}_\beta} + \delta t \sum_{j=0}^{i} \psi_j C_j^{\mathrm{B}_\alpha^+\dot{\mathrm{P}}} C_{i-j}^{\mathrm{PB}_\beta}/C_0^{\mathrm{PP}}\,, \tag{40}$$

with $C_0^{\mathrm{B}_\alpha^+\mathrm{B}_\beta^+} = C_0^{\mathrm{B}_\alpha\mathrm{B}_\beta}$. Eventually, higher-order integration methods than the trapezoidal rule could achieve better numerical stability when needed[29]. Note that, even for the projected auto-correlation function $C^{\mathrm{B}_\alpha^+\mathrm{B}_\alpha^+}(t)$, the projected cross-correlation function $C^{\mathrm{B}_\alpha^+\dot{\mathrm{P}}}(t)$ is needed.

Additionally, for numerical reasons or if one are only interested in the integral of the projected correlation functions, say $\Gamma^{\mathrm{B}_\alpha^+\mathrm{B}_\beta^+}(t) = \int_0^t C^{\mathrm{B}_\alpha^+\mathrm{B}_\beta^+}(t')\mathrm{d}t'$, the set of Volterra equations (Eqs. 37 and 38) can be integrated in time, using that $\int_0^t \mathrm{d}t' \int_0^{t'} \mathrm{d}s = \int_0^t \mathrm{d}s \int_s^t \mathrm{d}t'$ after the change of variable $t - s \to s$, to obtain

$$\Gamma^{\mathrm{B}_\alpha^+\mathrm{B}_\beta^+}(t) = \Gamma^{\mathrm{B}_\alpha\mathrm{B}_\beta}(t) + \int_0^t \frac{\Gamma^{\mathrm{B}_\alpha^+\dot{\mathrm{P}}}(s)}{\langle \mathrm{P}(0)^2\rangle}\langle \mathrm{P}(t-s)\mathrm{B}_\beta(0)\rangle\,\mathrm{d}s \tag{41}$$

and

$$\Gamma^{\mathrm{B}_\alpha^+\dot{\mathrm{P}}}(t) = \Gamma^{\mathrm{B}_\alpha\dot{\mathrm{P}}}(t) + \int_0^t \frac{\Gamma^{\mathrm{B}_\alpha^+\dot{\mathrm{P}}}(s)}{\langle \mathrm{P}(0)^2\rangle}\langle \mathrm{P}(t-s)\dot{\mathrm{P}}(0)\rangle\,\mathrm{d}s \tag{42}$$

where the two changes of variable $t'-s \to t'$ and $t-s \to s$ have been made. Those two sets of Volterra equations retain the exact same structure as Eqs. 37 and 38 and can thus be numerically evaluated with the same algorithm (Eqs. 39 and 40) but with different initial conditions given by $\Gamma^{\mathrm{B}_\alpha^+\dot{\mathrm{P}}}(0) = \Gamma^{\mathrm{B}_\alpha^+\mathrm{B}_\beta^+}(0) = 0$. Eventually, the projected correlation functions can then be obtained by numerical differentiation. The corresponding algorithms derived from the backward orthogonal dynamics given by Eq. 28 are provided in appendix A for completeness. The Volterra Eqs. 37 and 38 with the inversion algorithm Eqs. 39 and 40 are the main results of this paper.

III. MOLECULAR DYNAMICS CALCULATIONS OF A BULK LENNARD-JONES FLUID

A. Model

In order to test the numerical strategy just introduced, we investigate the self-diffusion of a bulk LJ fluid by looking into the contributions of the repulsive and attractive parts of the particles' interactions to the memory kernel. The LJ interaction potential U is written as a function of the inter-particle distance r as

$$U(r) = 4\epsilon \left[\left(\frac{\sigma}{r}\right)^{12} - \left(\frac{\sigma}{r}\right)^{6} \right], \tag{43}$$

with ϵ the depth of the potential well located at a distance $r_{\min} = 2^{1/6}\sigma$ that separates the interaction potential into a purely repulsive part, for $r \leq r_{\min}$, and an attractive one, for $r \geq r_{\min}$. Then, the total force f felt by a particle can be written as $f = f_{\rm r} + f_{\rm a}$, leading to the same decomposition for the noise, $\eta(t) = \mathrm{e}^{i\mathcal{Q}\mathcal{L}t} f(0) = \eta_{\rm r}(t) + \eta_{\rm a}(t)$. The memory kernel (Eq. 12) can be further decomposed as

$$k(t) = k_{\text{r-r}}(t) + k_{\text{a-a}}(t) + 2k_{\text{r-a}}(t)\,, \tag{44}$$

where the components of the memory kernel are defined as $k_{\text{x-y}}(t) = \langle\, \eta_{\rm x}(t)\eta_{\rm y}(0)\rangle\, /(k_BT)$ and are numerically evaluated from Eqs. 39 and 40 by identifying the set of observables $(\mathrm{B}_\alpha)_{\alpha\in[1,n_{\rm o}]} = (f_{\rm r}, f_{\rm a})$. Recalling that $\mathrm{P} = v$ and thus $\dot{\mathrm{P}} = f/m$, the intermediate functions $C^{\mathrm{B}^+_\alpha \dot{\mathrm{P}}}(t) = C^{\eta_{\rm x} f}(t)/m$ required to evaluate the memory kernels' components correspond to the cross-correlations between the components of the noise and the total force, yielding another decomposition of the memory kernel as $k(t) = k_{\text{r-t}}(t) + k_{\text{a-t}}(t)$, with $k_{\text{x-t}}(t) = C^{\eta_{\rm x} f}(t)/(k_BT)$ and where we have used that $\eta(0) = f(0)$. Then, with the notations of this section and by recalling that $\langle v(0)^2\rangle = k_BT/m$, Eq. 37 reads

$$k_BT k_{\text{x-y}}(t) = C^{f_{\rm x} f_{\rm y}}(t) + \int_0^t k_{\text{x-t}}(s) C^{v f_{\rm y}}(t-s)\,\mathrm{d}s\,. \tag{45}$$

Besides, the friction coefficient γ, related to the self-diffusion coefficient D through the Einstein relation $D = k_BT/\gamma$, which corresponds to the time integral of the memory kernel can also be decomposed the same way, introducing the friction components $\gamma_{\text{x-y}} = \int_0^\infty k_{\text{x-y}}(t)\mathrm{d}t$ for which we consider the time evolution of the running integrals

$$\gamma_{\text{x-y}}(t) = \int_0^t k_{\text{x-y}}(s)\mathrm{d}s \tag{46}$$

in what follows. Additionally, we distinguish the contributions of the sole memory effects on the memory kernel and the friction coefficients, denoted by the superscript m, which are defined by $k^{\rm m}_{\text{x-y}}(t) = k_{\text{x-y}}(t) - C^{f_{\rm x} f_{\rm y}}(t)/(k_BT)$ and $\gamma^{\rm m}_{\text{x-y}} = \int_0^\infty k^{\rm m}_{\text{x-y}}(t)\,\mathrm{d}t$, respectively, with

$$k^{\rm m}_{\text{x-y}}(t) = \int_0^t k_{\text{x-t}}(s) \frac{C^{v f_{\rm y}}(t-s)}{k_BT}\,\mathrm{d}s \tag{47}$$

from Eq. 45. Since the integral of the total force auto-correlation function quickly goes to zero, only the memory effects' contributions remain in the total friction coefficient, resulting in the long-time limit to $\gamma = \gamma^{\rm m}_{\text{r-r}} + \gamma^{\rm m}_{\text{a-a}} + 2\gamma^{\rm m}_{\text{r-a}}$

B. Numerical Details

A system of 1000 LJ particles of mass m interacting within a cutoff distance of $6\,\sigma$ at a density of $0.5\,\sigma^{-3}$ has been first equilibrated in a cubic periodic box during $231\,\tau$, where $\tau = \sqrt{\frac{\epsilon}{m\sigma^2}}$, using MD in the canonical ensemble and with a timestep $\Delta t = 4.6\,10^{-4}\,\tau$ to reach an equilibrium temperature of $1.5\,\epsilon/k_B$. The Nosé-Hoover thermostat has been used with a time constant of $0.92\,\tau$. Then, 90 independent production runs of $231\,\tau$ in the microcanonical ensemble have been generated using different seeds to randomly initialize the velocities according to the Maxwell-Boltzmann distribution. The LAMMPS code[30] has been used to perform all the MD calculations. If not explicitly mentioned, all results have been averaged over the whole set of trajectories (90) by processing their total length ($231\,\tau$) at every timestep ($\delta t = \Delta t$). The error bars correspond to the 95 % confidence interval.

C. Numerical Results

To begin with, the running integrals of the projected correlation functions are reported in Fig. 1 for a single trajectory of $10\,\tau$ sampled every two timesteps ($\delta t = 2\Delta t$), showing that we obtain very similar results to those of Carof *et al.*[21] for the same statistics. As they first noticed, the main contribution is the purely repulsive one. Additionally, the main algorithm derived here is tested in Fig. 2 against the second-order accurate reconstruction algorithm, implemented following[28], for the running integrals of each component of the friction coefficient. We see from the purely attractive contribution and cross contribution that both algorithms give identical result. However, for the purely repulsive contribution, for which the memory effects contribute the most, the reconstruction algorithm results start to deviate from a plateau before $2\,\tau$. Fig. 3 confirms that the results obtained through inversion of the Volterra equations converge toward the right value for the total friction coefficient as evaluated via the Green-Kubo relation $D = \int_0^\infty \langle v(t)v(0)\rangle\,\mathrm{d}t$. We also see that the integral of the force auto-correlation function rapidly converges to zero, canceling its long-term contribution to the friction coefficient and leaving simply $\gamma = \gamma^{\rm m}$.

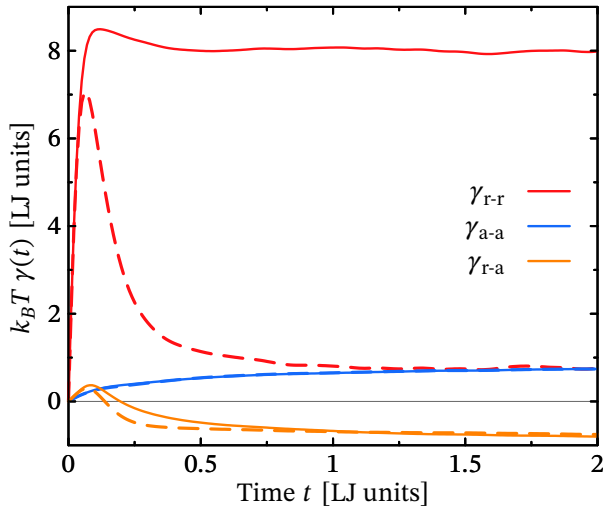

FIG. 1. Running time integrals of the projected correlation functions $k_BT\gamma_{\text{x-y}}(t)$ according to the repulsive-attractive decomposition of the potential (solid curves). The corresponding running integrals of the force correlation functions $\int_0^t C^{f_{\text{x}}f_{\text{y}}}(s)\mathrm{d}s$ are also shown (dashed lines). These results have been obtained for a single trajectory of 10τ with a time resolution of $2\Delta t$ for comparison with[21].

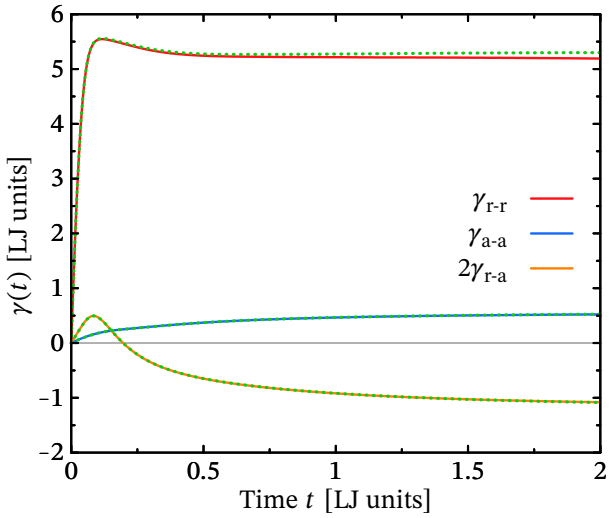

FIG. 2. Contributions to the friction coefficient (Eq. 46) according to the repulsive-attractive decomposition (Eq. 44) of the potential computed from the inversion of the Volterra equations (solid lines) and with the second-order FOD reconstruction method[28](green dotted lines). These results have been averaged over 30 independent trajectories of 231τ with a time resolution of Δt.

The running integrals of the friction coefficient $\gamma(t) = \gamma_{\text{r-t}}(t) + \gamma_{\text{a-t}}(t)$ corresponding to the intermediate projected correlation functions are also presented in Fig. 4 along with their force correlation counterparts, showing again that the repulsive interactions' contribution dominates friction in this case.

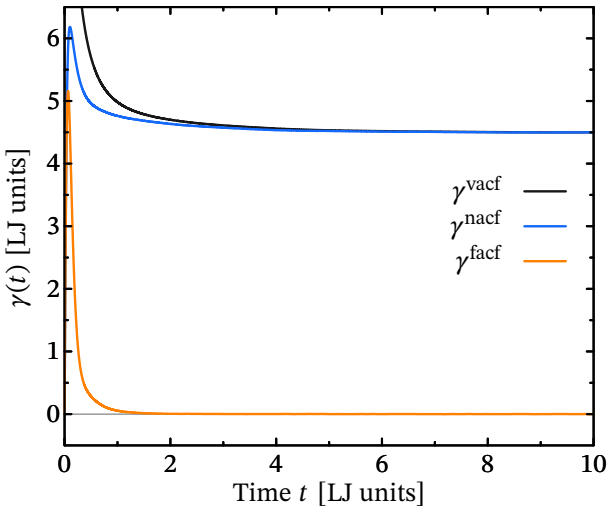

FIG. 3. Total friction coefficient obtained by integrating the total kernel Eq. 44 (blue), the velocity auto-correlation function as $k_BT/\int_0^t C^{vv}(s)\rangle\,\mathrm{d}s$ from Einstein and Green-Kubo relations (black), and the force auto-correlation function as $\int_0^t C^{ff}(s)\rangle\mathrm{d}s/(k_BT)$ (orange). The latter way amounts to ignoring the memory effects. These results have been averaged over 30 independent trajectories of 231τ with a time resolution of Δt.

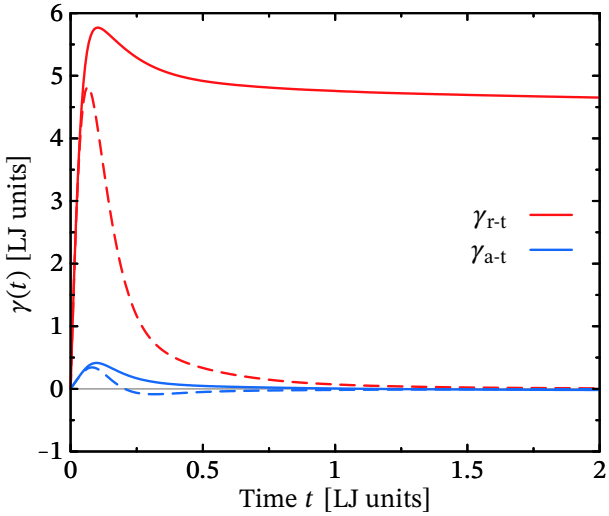

FIG. 4. Contributions to the friction coefficient (Eq. 46) corresponding to the partial decomposition $k(t) = k_{\text{r-t}}(t) + k_{\text{a-t}}(t)$ related to the intermediate projected correlation functions needed to perform the attractive-repulsive decomposition.

Thanks to the efficiency of the Volterra-based algorithms, the long-time decay of the memory kernel contributions can be investigated with a reasonable computational effort. The absolute values of the normalized memory kernels' components are shown in Figs. 5 and 6, where one notices that all the contributions display significant backscattering past a short time of around $0.1\,\tau$ except for the purely attractive kernel (blue line in Fig. 6)

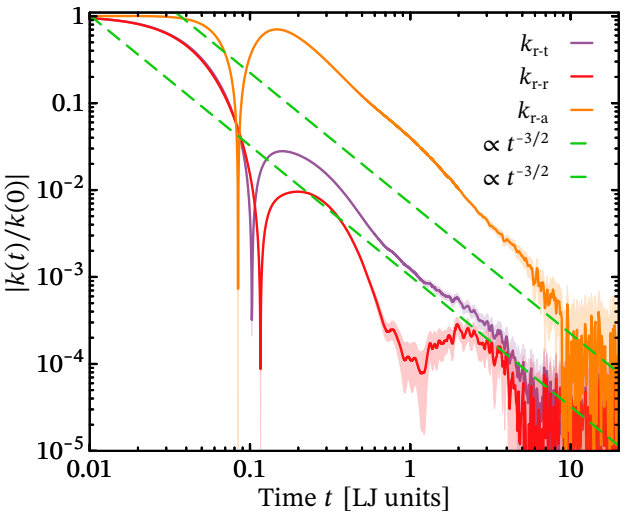

FIG. 5. Absolute values of the normalized memory kernels involving the repulsive part of the force (including the intermediate one $k_{\text{r-t}}$) following the repulsive-attractive decomposition of the force as functions of the time in logarithmic scales. The error bars indicated by the colored and translucent areas stand for the 95% confidence intervals.

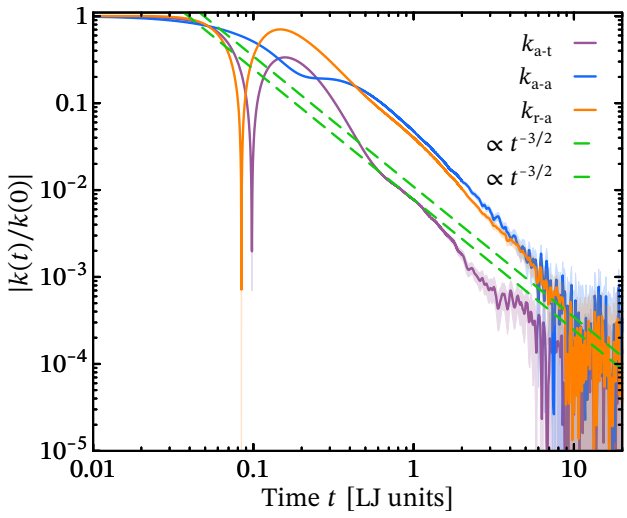

FIG. 6. Absolute values of the normalized memory kernels involving the attractive part of the force (including the intermediate one $k_{\text{a-t}}$) following the repulsive-attractive decomposition of the force.

that briefly plateaus before decaying to zero similarly to the other kernels. As the repulsive interactions dominate, this behavior is hidden in the attractive intermediate memory kernel $k_{\text{a-t}}(t)$ (violet line in Fig. 6). Interestingly, all the memory kernel contributions ultimately decay to zero in the long-time limit following the same scaling as $t^{-3/2}$, which corresponds to the long-time decay of the total memory kernel as first noted by[28] at the molecular scale in agreement with hydrodynamics for macroscopic colloids' diffusion[31]. This hydrodynamic scaling also applies to all the contributions of the memory kernel down to the molecular scale. In other words, no contribution decays faster than the total memory kernel, and none of these contributions is individually responsible for this scaling.

Coming back to the friction coefficient components (Fig. 7), we see that their long-time contributions, as calculated by the inversion of the Volterra equations introduced here, remain stable in the long-time limit. This is especially important in the case of the repulsive-attractive cross-correlation contribution $2\gamma_{\text{r-a}}$, which in fact clearly differs from its counterpart obtained from the corresponding force cross-correlations. This difference, which corresponds to the contribution of the memory effects $2\gamma^{\text{m}}_{\text{r-a}}$, despite being small, remains strictly negative, as evidenced by Fig. 8, as opposed to the purely attractive part, where memory effects barely arise at short times. These memory effects could not be detected by Carof *et al.*[21] as their results were relatively noisy. In addition, their study is limited to a maximum time of 2τ, which prevents observing the crossover and plateau behaviors of the attractive-repulsive memory effects that

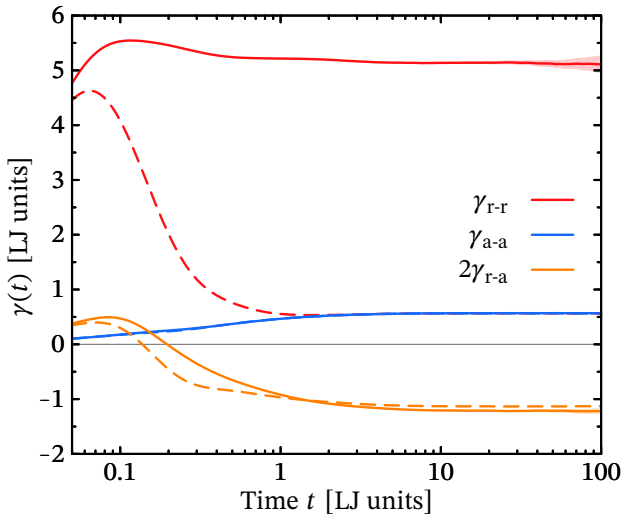

FIG. 7. Running time integrals of the projected correlation functions ($\gamma_{\text{x-y}}(t)$) according to the repulsive-attractive decomposition of the potential (solid curves) as functions of the time in logarithmic scale. The corresponding running integrals of the force correlation functions $\int_0^t C^{f_{\text{x}}f_{\text{y}}}(s)\text{d}s/(k_BT)$ are also shown (dashed lines).

are best illustrated in Fig. 8.

Computing such quantities from MD trajectories is clearly intensive, both in terms of memory and calculation. Since the method introduced here relies only on the inversion of Volterra equations, which can be efficiently done from correlation functions, reducing the amount of data to be saved during the MD calculations would prove to be convenient. This point is especially daunting when using the reconstruction algorithms because the same time resolution used to calculate the tra-

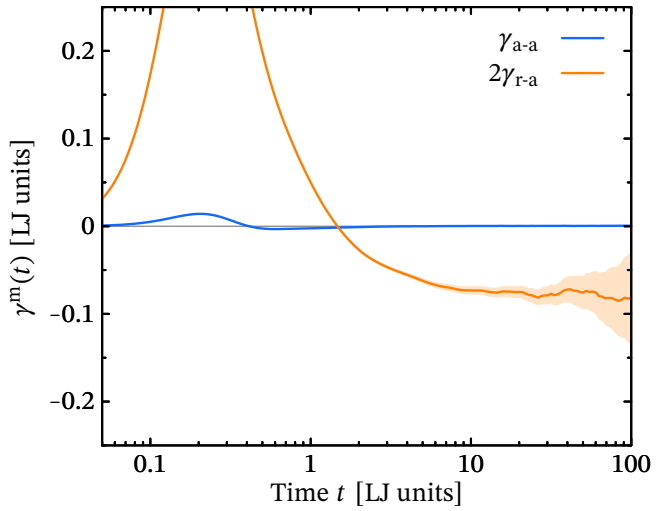

FIG. 8. Running integrals $\gamma^{\text{m}}_{\text{x-y}}(t) = \int_0^t k^{\text{m}}_{\text{x-y}}(s)\text{d}s$ of the memory effects' contributions to the components of the friction coefficient involving the attractive part of the potential.

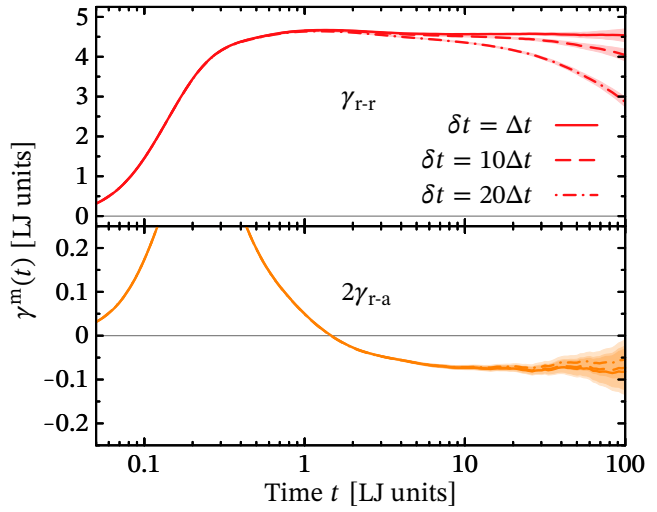

FIG. 9. Same as Fig. 8 but for various time resolutions and with separate windows for the two components.

jectories is needed ($\delta t = \Delta t$). We repeated the evaluation of the memory contributions related to the repulsive interactions by using lower time resolutions when processing the trajectories (Fig. 9). We see that the time resolution can be reasonably decreased to one tenth of the MD time resolution ($\delta t = 10\Delta t$) in order to evaluate the most sensitive plateau values of the different contributions. Going further could prevent one from even observing the plateaus, especially in the case of the purely repulsive contribution, which dominates friction. This is associated with the non-monotonous behavior of the anti-correlations arising before the ultimate long-term decay (Fig. 5).

All the results obtained here by solving the Volterra equations (Eqs. 37 and 38) have been identically reproduced by the inversion of the Volterra equations for the running integrals (Eqs. 41 and 42). On the contrary, the corresponding Volterra equations for the backward orthogonal dynamics derived in the appendix led to unstable algorithms while introducing no benefit compared to the ones of the FOD.

IV. CONCLUSIONS AND PERSPECTIVES

By deriving sets of Volterra equations of the second kind from the orthogonal dynamics for a collection of observables, one can reemploy the simple numerical inversion schemes of Volterra equations to obtain stable and efficient algorithms to compute projected cross-correlations. This strategy is numerically advantageous because the inputs required are the already averaged time correlation functions between the observables and the relevant variable and its time derivative, which can all be efficiently estimated via the Wiener-Khintchine theorem (or cross-correlation theorem).

Then, application to the decomposition of the memory kernel related to the diffusion of tagged particles in a bulk LJ fluid allowed investigation of the long-term behavior of the diffusive dynamics to show that the memory effects of the cross-correlations between the repulsive and attractive interactions between LJ particles give a small but persistent contribution to the total friction coefficient. Interestingly, it has been shown that the decay of each memory kernel contribution follows the algebraic decay predicted by hydrodynamics for the diffusion of macroscopic colloids. We saw that decreasing the time resolution of the trajectory post-processing can be effectively done without significant impact on the accuracy, but care must be taken when dealing with cross-correlations that exhibit complex behavior, especially if one is interested in their time integrals.

Beyond being useful in practice to further simplify the study of more complex dynamics than bulk LJ fluids, such as confined fluid molecules, the strategy presented here could be reused for non-linear[32–34] or non-stationary GLEs[35–38].

CONFLICTS OF INTEREST

The author has no conflict to disclose.

DATA AVAILABILITY STATEMENT

The data that support the findings of this study are available from the corresponding author upon reasonable request.

Appendix A: Volterra Equations for the Backward Orthogonal Dynamics

Using Eq. 28 for B_α and taking its average after multiplying by $\mathrm{B}^-_\beta(0) = \mathrm{B}_\beta(0)$ one arrives to

$$\langle \mathrm{B}^-_\alpha(t)\mathrm{B}^-_\beta(0)\rangle = \langle \mathrm{B}_\alpha(-t)\mathrm{B}_\beta(0)\rangle + \int_0^t \frac{\langle \mathrm{B}^-_\alpha(s)\mathrm{P}(0)\rangle}{\langle \mathrm{P}(0)^2\rangle}\langle \dot{\mathrm{P}}(s-t)\mathrm{B}_\beta(0)\rangle\,\mathrm{d}s \quad \text{(A1)}$$

which are also Volterra equations of the second kind. The same step is repeated with $\mathrm{P}(0)$ to get Volterra equations for $C^{\mathrm{B}^-_\alpha\mathrm{P}}(t)$ as

$$\langle \mathrm{B}^-_\alpha(t)\mathrm{P}(0)\rangle = \langle \mathrm{B}_\alpha(-t)\mathrm{P}(0)\rangle + \int_0^t \frac{\langle \mathrm{B}^-_\alpha(s)\mathrm{P}(0)\rangle}{\langle \mathrm{P}(0)^2\rangle}\langle \dot{\mathrm{P}}(s-t)\mathrm{P}(0)\rangle\,\mathrm{d}s\,. \quad \text{(A2)}$$

The correlation functions appearing in the two previous equations are stationary because B_α and $\dot{\mathrm{P}}$ are Hamiltonian dynamical quantities, then we have $C^{\mathrm{B}_\alpha\mathrm{B}_\beta}(-t) = C^{\mathrm{B}_\beta\mathrm{B}_\alpha}(t)$ as well as $C^{\mathrm{B}_\alpha\mathrm{P}}(-t) = C^{\mathrm{P}\mathrm{B}_\alpha}(t)$. These Volterra equations can be numerically solved as

$$C_i^{\mathrm{B}^-_\alpha\mathrm{P}} = C_i^{\mathrm{P}\mathrm{B}_\alpha} + \delta t\sum_{j=0}^{i-1}\psi_j C_j^{\mathrm{B}^-_\alpha\dot{\mathrm{P}}} C^{\mathrm{P}\dot{\mathrm{P}}}_{j-i}/C_0^{\mathrm{P}\mathrm{P}}\,, \quad \text{(A3)}$$

since $C_0^{\mathrm{P}\dot{\mathrm{P}}} = 0$, following the same procedure as for Eq. 15. Then, Eq. A1 can be numerically integrated as

$$C_i^{\mathrm{B}^-_\alpha\mathrm{B}^-_\beta} = C_i^{\mathrm{B}_\beta\mathrm{B}_\alpha} + \delta t\sum_{j=0}^{i}\psi_j C_j^{\mathrm{B}^-_\alpha\dot{\mathrm{P}}} C^{\dot{\mathrm{P}}\mathrm{B}_\beta}_{j-i}/C_0^{\mathrm{P}\mathrm{P}} \quad \text{(A4)}$$

with the trapezoidal rule and the initial step $C_0^{\mathrm{B}^-_\alpha\mathrm{B}^-_\beta} = C_0^{\mathrm{B}_\beta\mathrm{B}_\alpha}$.

Then, following the same steps to go from Eqs. 37 and 38 to Eqs. 41 and 42 lead to the integral form of the two previous Volterra equations as

$$\Gamma^{\mathrm{B}^-_\alpha\mathrm{B}^-_\beta}(t) = \Gamma^{\mathrm{B}_\alpha\mathrm{B}_\beta}(t) + \int_0^t \frac{\Gamma^{\mathrm{B}^-_\alpha\mathrm{P}}(s)}{\langle \mathrm{P}(0)^2\rangle}\langle \dot{\mathrm{P}}(s-t)\mathrm{B}_\beta(0)\rangle\,\mathrm{d}s \quad \text{(A5)}$$

and

$$\Gamma^{\mathrm{B}^-_\alpha\mathrm{P}}(t) = \Gamma^{\mathrm{B}_\alpha\mathrm{P}}(-t) + \int_0^t \frac{\Gamma^{\mathrm{B}^-_\alpha\mathrm{P}}(s)}{\langle \mathrm{P}(0)^2\rangle}\langle \dot{\mathrm{P}}(s-t)\mathrm{P}(0)\rangle\,\mathrm{d}s \quad \text{(A6)}$$

which again keep the same structure as Eqs. A1 and A2 allowing us to solve them with the same algorithm (Eqs. A3 and A4) with different initial conditions $\Gamma^{\mathrm{B}^-_\alpha\mathrm{P}}(0) = \Gamma^{\mathrm{B}^-_\alpha\mathrm{B}^-_\beta}(t) = 0$.

[1] R. Zwanzig, Physical Review **124**, 983 (1961).
[2] H. Mori, Progress of Theoretical Physics **33**, 423 (1965).
[3] R. Zwanzig, *Nonequilibrium statistical mechanics* (Oxford university press, 2001).
[4] B. J. Berne and G. D. Harp, *Advances in Chemical Physics* (John Wiley & Sons, Ltd, 1970).
[5] S. S. Cohen and R. E. Wilde, The Journal of Chemical Physics **68**, 1138 (1978).
[6] M. Berkowitz, J. D. Morgan, D. J. Kouri, and J. A. McCammon, The Journal of Chemical Physics **75**, 2462 (1981).
[7] D. Gordon, V. Krishnamurthy, and S.-H. Chung, The Journal of Chemical Physics **131**, 134102 (2009).
[8] H. K. Shin, C. Kim, P. Talkner, and E. K. Lee, Chemical Physics **375**, 316 (2010).
[9] C. Kim and G. E. Karniadakis, Journal of Statistical Physics **158**, 1100 (2015).
[10] J. O. Daldrop, B. G. Kowalik, and R. R. Netz, Physical Review X **7** (2017).
[11] J. O. Daldrop, J. Kappler, F. N. Brünig, and R. R. Netz, Proceedings of the National Academy of Sciences **115**, 5169 (2018).
[12] B. Kowalik, J. O. Daldrop, J. Kappler, J. C. F. Schulz, A. Schlaich, and R. R. Netz, Physical Review E **100** (2019).
[13] J. O. Daldrop and R. R. Netz, The Journal of Physical Chemistry B **123**, 8123 (2019).
[14] Y. Han, J. Jin, and G. A. Voth, The Journal of Chemical Physics **154**, 084122 (2021).
[15] G. R. Kneller and K. Hinsen, The Journal of Chemical Physics **115**, 11097 (2001).
[16] C. Hijón, P. Español, E. Vanden-Eijnden, and R. Delgado-Buscalioni, Faraday Discussions **144**, 301 (2009).
[17] E. Darve, J. Solomon, and A. Kia, Proceedings of the National Academy of Sciences **106**, 10884 (2009).
[18] D. Kauzlarić, P. Español, A. Greiner, and S. Succi, Macromolecular Theory and Simulations **20**, 526 (2011).
[19] G. Jung, M. Hanke, and F. Schmid, Journal of chemical theory and computation **13**, 2481 (2017).
[20] H. Vroylandt, L. Goudenège, P. Monmarché, F. Pietrucci, and B. Rotenberg, Proceedings of the National Academy of Sciences **119**, e2117586119 (2022).
[21] A. Carof, R. Vuilleumier, and B. Rotenberg, The Journal of chemical physics **140**, 124103 (2014).
[22] A. Carof, V. Marry, M. Salanne, J.-P. Hansen, P. Turq, and B. Rotenberg, Molecular Simulation **40**, 237 (2014).
[23] M. te Vrugt and R. Wittkowski, European Journal of Physics **41**, 045101 (2020).
[24] A. Khintchine, Mathematische Annalen **109**, 604 (1934).
[25] V. Calandrini, E. Pellegrini, P. Calligari, K. Hinsen, and G. Kneller, École thématique de la Société Française de la Neutronique **12**, 201 (2011).
[26] D. Givon, R. Kupferman, and O. H. Hald, Israel Journal of Mathematics **145**, 221 (2005).
[27] Duhamel's principle gives the solution to an inhomogeneous initial value problem $\dot{u}(t) - Du(t) = F(t)$, with $u(0) = u_0$ for a time-independent operator D and a function F as $u(t) = \mathrm{e}^{Dt}u_0 + \int_0^t \mathrm{e}^{D(t-s)}F(s)\mathrm{d}s$. Identifying $u = \mathrm{M}^+$, $D = i\mathcal{L}$ and $F = -\mathcal{P}i\mathcal{L}\mathrm{M}^+$ from Eq. 21 straightforwardly shows that Eq. 27 derives from Duhamel's principle, which is equivalent to applying Dyson's identity (Eq. 6) to $\mathrm{M}(0)$. Similarly, Eq. 28 derives from Duhamel's principle ($u = \mathrm{N}^-$, $D = -i\mathcal{L}$ and $F = i\mathcal{L}\mathcal{P}\mathrm{N}^-$) in agreement with the corresponding Dyson identity (Eq. 30).
[28] D. Lesnicki, R. Vuilleumier, A. Carof, and B. Rotenberg, Phys. Rev. Lett. **116**, 147804 (2016).
[29] P. Linz, SIAM studies in applied mathematics (1985).
[30] A. P. Thompson, H. M. Aktulga, R. Berger, D. S. Bolintineanu, W. M. Brown, P. S. Crozier, P. J. in 't Veld, A. Kohlmeyer, S. G. Moore, T. D. Nguyen, R. Shan, M. J. Stevens, J. Tranchida, C. Trott, and S. J. Plimpton, Comp. Phys. Comm. **271**, 108171 (2022).
[31] N. Corngold, Physical Review A **6**, 1570 (1972).
[32] H. Vroylandt and P. Monmarché, The Journal of Chemical Physics **156**, 244105 (2022).

[33]H. Vroylandt, Europhysics Letters **140**, 62003 (2022).
[34]C. Ayaz, L. Scalfi, B. A. Dalton, and R. R. Netz, Physical Review E **105**, 054138 (2022).
[35]S. Kawai and T. Komatsuzaki, The Journal of Chemical Physics **134**, 114523 (2011).
[36]H. Meyer, T. Voigtmann, and T. Schilling, The Journal of Chemical Physics **147**, 214110 (2017).
[37]H. Meyer, P. Pelagejcev, and T. Schilling, EPL (Europhysics Letters) **128**, 40001 (2020).
[38]C. Widder, F. Koch, and T. Schilling, The Journal of Chemical Physics **157**, 194107 (2022).